

Contrastive Deep Graph Clustering with Learnable Augmentation

Xihong Yang, Yue Liu, Sihang Zhou, Siwei Wang, Xinwang Liu, En Zhu

Abstract—Graph contrastive learning is an important method for deep graph clustering. The existing methods first generate the graph views with stochastic augmentations and then train the network with a cross-view consistency principle. Although good performance has been achieved, we observe that the existing augmentation methods are usually random and rely on pre-defined augmentations, which is insufficient and lacks negotiation between the final clustering task. To solve the problem, we propose a novel **Graph Contrastive Clustering** method with the **Learnable graph Data Augmentation** (GCC-LDA), which is optimized completely by the neural networks. An adversarial learning mechanism is designed to keep cross-view consistency in the latent space while ensuring the diversity of augmented views. In our framework, a structure augmentor and an attribute augmentor are constructed for augmentation learning in both structure level and attribute level. To improve the reliability of the learned affinity matrix, clustering is introduced to the learning procedure and the learned affinity matrix is refined with both the high-confidence pseudo-label matrix and the cross-view sample similarity matrix. During the training procedure, to provide persistent optimization for the learned view, we design a two-stage training strategy to obtain more reliable clustering information. Extensive experimental results demonstrate the effectiveness of GCC-LDA on six benchmark datasets.

Index Terms—Graph Node Clustering; Contrastive Learning; Graph Neural Network; Learnable Augmentation

1 INTRODUCTION

IN recent years, graph learning methods [1], [2], [3], [4], [5] have attracted considerable attention in various applications, e.g., node classification [6], [7], [8], Graph Anomaly Detection [9], collaborative filtering [10], [11], molecular graph [12], [13], recommendation [14], [15], [16] etc. Among all directions, deep graph clustering [17], [18], [19], [20], [21], which aims to encode nodes with neural networks and divide them into disjoint clusters without manual labels, has become a hot research spot.

With the strong capability of capturing implicit supervision, contrastive learning has become an important technique in deep graph clustering. In general, the existing methods first generate augmented graph views by perturbing node connections or attributes, and then keep the same samples in different views consistent while enlarging the difference between distinct samples. Although verified effective, we find that the performance of the existing contrastive methods [18], [22], [23] heavily depends on the quality of random augmentation operations, leading to the uncertain performance. To alleviate the problem, in graph classification, JOAO [24] selects a proper augmentation type among several pre-defined candidates. Although better performance is achieved, the specific augmentation process is still based on the pre-defined schemes and is not learnable. To fill this gap, AD-GCL [25] proposes a learnable augmentation scheme to drop edges according to Bernoulli distribution, while neglecting augmentations on node attributes. More recently, AutoGCL [26] proposes an auto augmentation strategy to mask or drop nodes via learning a probability distribution. A large step is made by these algorithms by proposing learnable augmentation. However, these strategies only focus on exploring augmentation over affinity matrixes while neglecting the learning of good attribute augmentations. Moreover, previous methods isolate the representation learning process

with the downstream tasks, making the learned representation less suitable to the final learning task, degrading the algorithm performance.

To solve these issues, we propose a fully learnable augmentation strategy for deep contrastive clustering in both structure and attribute levels. Especially, we design an adversarial mechanism to keep the cross-view consistency in the latent space while ensuring the diversity of augmented views. To be specific, we design the structure and attribute augmenters to learn the structure and attribute information dynamically, thus avoiding the complex and random selections of the existing and pre-defined augmentations. In addition, we refine the learned structure with the high-confidence clustering pseudo-label matrix and the cross-view sample similarity matrix. Moreover, during the model training, we present a two-stage training strategy to obtain reliable clustering information.

By these settings, we integrate the clustering task and the augmentation learning into the unified framework. Firstly, the high-quality augmented graph improves the discriminative capability of embeddings, thus better assisting the clustering task. Meanwhile, the high-confidence clustering results are utilized to refine the augmented graph structure. Concretely, samples within the same clusters are more likely to link. Differently, we remove the edges between samples from different clusters. The key contributions of this paper are listed as follows:

- We propose a fully learnable data augmentation framework for deep contrastive clustering, termed GCC-LDA, by designing the structure and attribute augmentor to dynamically learn the structure and attribute information.
- Under clustering guidance, GCC-LDA refines the augmented graph structure with the cross-view similarity matrix and high-confidence pseudo label matrix.
- The clustering task and the augmentation learning are integrated into the unified framework and promote each other.

- Extensive experimental results have demonstrated that GCC-LDA outperforms the existing state-of-the-art deep graph clustering competitors.

2 RELATED WORK

2.1 Contrastive Deep Graph Clustering

Clustering is to divide nodes into disjoint clusters [27], [28], [29], [30], [31], [32], [33], [34], [35]. Among those methods, deep graph clustering has attracted great attention in recent years. The existing deep graph clustering methods can be roughly categorized into three classes: generative methods [17], [19], [21], [36], [37], [38], [39], [40], adversarial methods [20], [41], [42], and contrastive methods [18], [22], [23], [43], [44], [45]. More details of deep graph clustering can be found in this survey paper [46]. In recent years, the contrastive learning has achieved great success in vision [47], [48], [49], [50] and graph [5], [51], [52], [53], [54], [55]. In this paper, we focus on the data augmentation of the contrastive deep graph clustering methods. Concretely, a pioneer AGE [43] conducts contrastive learning by a designed adaptive encoder. Besides, MVGRL [22] generates two augmented graph views. Subsequently, DCRN [18] and IDCRN [56] aim to alleviate the collapsed representation by reducing correlation in both sample and feature levels. Meanwhile, the positive and negative sample selection have attracted great attention of researchers. Concretely, GDCL [23] develops a debiased sampling strategy to correct the bias for negative samples. Although promising performance has been achieved, previous methods generate different graph views by adopting uniform data augmentations like graph diffusion, edge perturbation, and feature disturbance. Moreover, these augmentations are manually selected and can not be optimized by the network, thus limiting the performance. To solve this problem, we propose a novel contrastive deep graph clustering framework with learnable graph data augmentations.

2.2 Data Augmentation in Graph Contrastive Learning

Graph data augmentation [57], [58], [59] is a important component of contrastive learning. The existing data augmentation methods in graph contrastive learning could rough divide into three categories, i.e. augment-free methods [60], adaptive augmentation methods [24], [61], [62], and learnable data augmentation methods [25], [26], [63]. AFGRL [60] generates the alternative view by discovering nodes that have local and global information without augmentation. While the diversity of the constructed view is limited, leading to poor performance. Furthermore, to make graph augmentation adaptive to different tasks, JOAO [24] learns the sampling distribution of the pre-defined augmentation to automatically select data augmentation. GCA [61] proposed an adaptive augmentation with incorporating various priors for topological and semantic aspects of the graph. However, the augmentation is still not learnable in the adaptive augmentation methods. Besides, in the field of graph classification, AD-GCL [25] proposed a learnable augmentation for edge-level while neglecting the augmentations on the node level. More recently, AutoGCL [26] proposed a probability-based learnable augmentation. Although promising performance has achieved, the previous methods still rely on the existing and pre-defined data augmentations. In this work, we propose a fully learnable augmentation strategy. Compared with the existing algorithms, GCC-LDA could generate the augmented view via a learnable way in both structure and attribute level. The

Table 1: Notation summary.

Notation	Meaning
$\mathbf{X} \in \mathbb{R}^{N \times D}$	Attribute matrix
$\mathbf{A} \in \mathbb{R}^{N \times N}$	Original adjacency matrix
$\mathbf{D} \in \mathbb{R}^{N \times N}$	Degree matrix
$\mathbf{E}^{v_k} \in \mathbb{R}^{N \times d}$	Node embeddings in k -th view
$\varphi(\cdot)$	Non-parametric metric function
$\mathbf{S} \in \mathbb{R}^{N \times N}$	Similarity sample matrix
$\mathbf{Z} \in \mathbb{R}^{N \times N}$	High-confidence pseudo label matrix
$\mathbf{Aug}_x \in \mathbb{R}^{N \times d}$	Augmented attribute matrix
$\mathbf{Aug}_s \in \mathbb{R}^{N \times N}$	Augmented structure matrix

discriminative capacity of the network could be improved by the learnable augmentation.

3 METHOD

In this section, we propose a novel Graph Contrastive Clustering method with Learnable Data Augmentation (GCC-LDA). The overall framework of GCC-LDA is shown in Fig.1. The main components in the proposed method include the learnable graph augmentation module and the reliable refinement module. We will detail the proposed GCC-LDA in the following subsections.

3.1 Notations Definition

For an undirected graph $\mathbf{G} = \{\mathbf{X}, \mathbf{A}\}$. $\mathbf{X} \in \mathbb{R}^{N \times D}$ is the attribute matrix, and $\mathbf{A} \in \mathbb{R}^{N \times N}$ represents the original adjacency matrix. $\mathbf{D} = \text{diag}(d_1, d_2, \dots, d_N) \in \mathbb{R}^{N \times N}$ is denoted as the degree matrix, where $d_i = \sum_{(v_i, v_j) \in \mathcal{E}} a_{ij}$. The normalized graph Laplacian matrix $\mathbf{L} = \mathbf{D} - \mathbf{A}$ is denoted as $\tilde{\mathbf{L}} = \hat{\mathbf{D}}^{-\frac{1}{2}} \hat{\mathbf{L}} \hat{\mathbf{D}}^{-\frac{1}{2}}$. Moreover, we define $\varphi(\cdot)$ is a non-parametric metric function to calculate pair-wise similarity, e.g. cosine similarity function. \mathbf{Aug}_A and \mathbf{Aug}_x represent the augmented structure and attribute matrix, respectively. The basic notations are summarized in Table 1.

3.2 Learnable Graph Augmentation Module

In this subsection, we propose a learnable graph augmentation strategy in both structure and attribute level. To be specific, we design the structure augmentor and attribute augmentor to dynamically learn the structure and attribute, respectively. In the following, we will introduce these augmentors in detail.

MLP-based Structure Augmentor The structure \mathbf{Aug}_s is learned by the Multi-Layer Perception in MLP structure augmentor as follows:

$$\mathbf{A}_{MLP} = \varphi(\mathbf{E}) = \varphi(MLP(\mathbf{A})), \quad (1)$$

where $\mathbf{E} \in \mathbb{R}^{N \times D}$ is the embedding of the original adjacency. Here, we adopt the cosine similarity function as $\varphi(\cdot)$ to calculate the learned structure matrix \mathbf{A}_{MLP} .

GCN-based Structure Augmentor GCN-based structure generator embeds the attribute matrix \mathbf{X} and original adjacency matrix \mathbf{A} into embeddings in the latent space. For simplicity, we define the GCN-based structure augmentor as:

$$\mathbf{A}_{GCN} = \varphi(\mathbf{E}) = \sigma(\tilde{\mathbf{D}}^{-\frac{1}{2}} \tilde{\mathbf{A}} \tilde{\mathbf{D}}^{-\frac{1}{2}} \mathbf{X}), \quad (2)$$

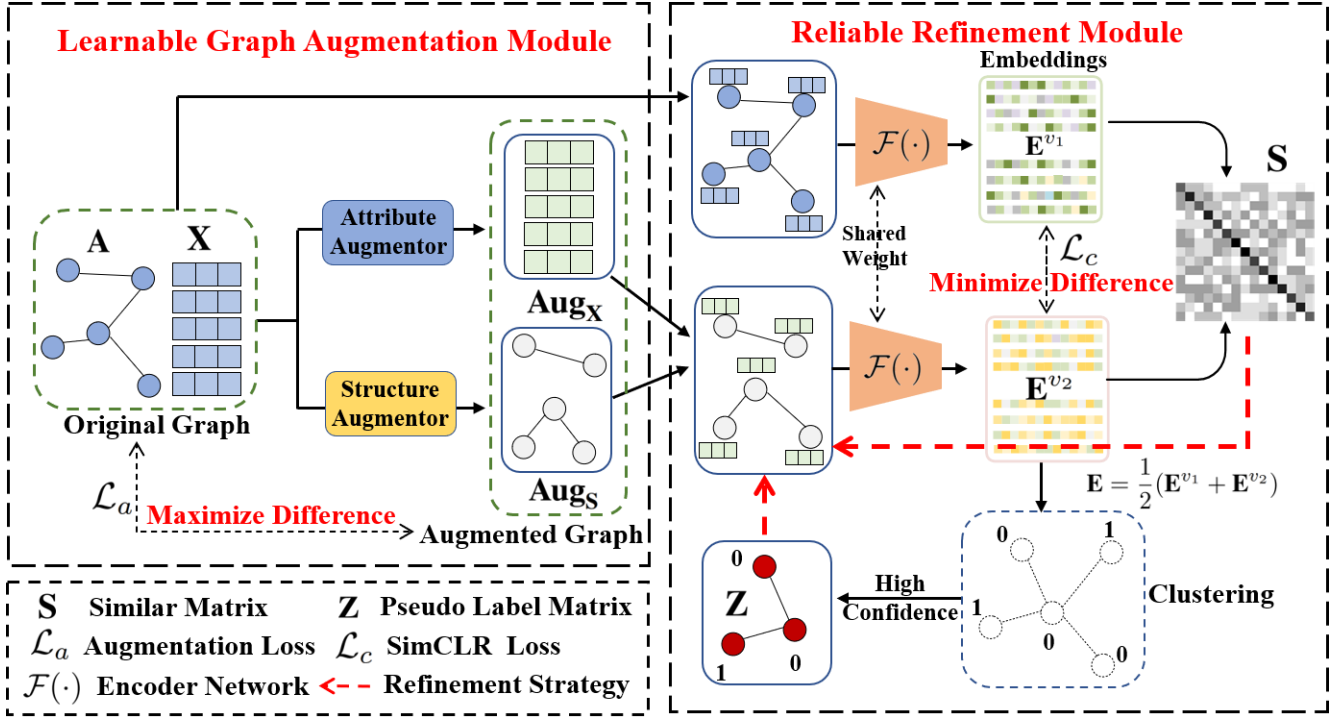


Figure 1: Illustration of the learnable augmentation algorithm for graph contrastive clustering. In our proposed algorithm, an adversarial learning mechanism is designed to keep cross-view consistency in the latent space while ensuring the diversity of augmented views. Besides, we design the structure and attribute augmentor to dynamically learn the structure and attribute information, respectively. Moreover, we optimize the structure of the augmented view with two aspects. Specifically, on the one hand, with the two-stage training strategy, we obtain the high-confidence clustering pseudo label matrix \mathbf{Z}_{ij} . On the other, we calculate the cross-view similarity matrix \mathbf{S}_{ij} to reflect the node’s adjacency relationship. After that, we refine the learnable structure \mathbf{Aug}_S with \mathbf{Z}_{ij} and \mathbf{S}_{ij} , thus integrating the clustering task and the augmentation learning into the unified framework.

similar to Eq.1, \mathbf{E} is embedding extracted by the GCN network, e.g. GCN [6], GCN-Cheby [64]. $\sigma(\cdot)$ is a non-linear operation.

Attention-based Structure Augmentor Inspire by GAT [7], we design an attentive network to capture the important structure of the input graph \mathbf{G} . To be specific, the normalized attention coefficient matrix $\mathbf{A}_{att_{ij}}$ between node x_i and x_j could be computed as:

$$\begin{aligned} \mathbf{A}_{att_{ij}} &= \bar{\mathbf{n}}^T (\mathbf{W}_{x_i} \parallel \mathbf{W}_{x_j}), \\ \mathbf{A}_{att_{ij}} &= \frac{e^{(\mathbf{A}_{att_{ij}})}}{\sum_{k \in \mathcal{N}_i} e^{(\mathbf{A}_{att_{ik}})}}, \end{aligned} \quad (3)$$

where $\bar{\mathbf{n}}$ and \mathbf{W} is the learnable weight vector and weight matrix, respectively. \parallel is the concatenation operation between the weight matrix \mathbf{W}_{x_i} and \mathbf{W}_{x_j} , and \mathcal{N}_i represents the indices the neighbors of node x_i . By this setting, the model could preserve important topological and semantic graph patterns via the attention mechanism.

To make the augmented view in a fully learnable manner, we design the attribute augmentor to dynamically learn the original attribute.

MLP-based Attribute Augmentor Similar to the MLP-based structure augmentor, we utilize the Multi-Layer Perception (MLP) as the network to learn the original attribute matrix \mathbf{X} . The learned attribute matrix $\mathbf{Aug}_X \in \mathbb{R}^{N \times D}$ can be presented as:

$$\mathbf{X}_{MLP} = MLP(\mathbf{X}). \quad (4)$$

where $MLP(\cdot)$ is the MLP network to learn the attribute.

Attention-based Attribute Augmentor To guide the network to take more attention to the important node attributes, we also design an attention-based attribute augmentor. Specifically, we map the node attributes into three different latent spaces:

$$\begin{aligned} \mathbf{Q} &= \mathbf{W}_q \mathbf{X}^T \\ \mathbf{K} &= \mathbf{W}_k \mathbf{X}^T \\ \mathbf{V} &= \mathbf{W}_v \mathbf{X}^T \end{aligned} \quad (5)$$

where $\mathbf{W}_q \in \mathbb{R}^{D \times D}$, $\mathbf{W}_k \in \mathbb{R}^{D \times D}$, $\mathbf{W}_v \in \mathbb{R}^{D \times D}$ are the learnable parameter matrices. And $\mathbf{Q} \in \mathbb{R}^{D \times N}$, $\mathbf{K} \in \mathbb{R}^{D \times N}$ and $\mathbf{V} \in \mathbb{R}^{D \times N}$ denotes the query matrix, key matrix and value matrix, respectively.

The attention-based attribute matrix \mathbf{Aug}_X can be calculated by:

$$\mathbf{Aug}_X = softmax\left(\frac{\mathbf{K}^T \mathbf{Q}}{\sqrt{D}}\right) \mathbf{V}^T, \quad (6)$$

After the structure augmentor and attribute augmentor, we could obtain the augmented view $\mathbf{G}^{v2} = (\mathbf{Aug}_S, \mathbf{Aug}_X)$, which is fully learnable.

3.3 Reliable Refinement Module

In this subsection, we firstly embed the node into the latent space through Eq.7:

$$\mathbf{E} = \mathcal{F}(\mathbf{G}), \quad (7)$$

where $\mathcal{F}(\cdot)$ denotes the encoder of our feature extraction framework. Subsequently, we obtain the embeddings of the original view \mathbf{G}^{v_1} and the augmented view \mathbf{G}^{v_2} with ℓ^2 -norm as follows:

$$\begin{aligned}\mathbf{E}^{v_1} &= \mathcal{F}(\mathbf{G}^{v_1}); \\ \mathbf{E}^{v_2} &= \mathcal{F}(\mathbf{G}^{v_2}),\end{aligned}\quad (8)$$

In the following, we fuse the two views of the node embeddings as follows:

$$\mathbf{E} = \frac{1}{2}(\mathbf{E}^{v_1} + \mathbf{E}^{v_2}). \quad (9)$$

Then we perform K-means [65] on \mathbf{E} and obtain the clustering results. After that, we will refine the learned view in two manners, i.e. similarity matrix and pseudo labels matrix refinement.

Similarity Matrix Refinement Through $\mathcal{F}(\cdot)$, we could obtain the embeddings of each view. Subsequently, the similarity matrix \mathbf{S} represents the similarity between i -th sample in the first view and j -th sample in the second view as formulated:

$$\mathbf{S}_{ij} = (\mathbf{E}_i^{v_1})^T \mathbf{E}_j^{v_2}, i, j \in [1, 2, \dots, N], \quad (10)$$

where \mathbf{S}_{ij} is the cross-view similarity matrix. The proposed similarity matrix \mathbf{S} measures the similarity between samples by comprehensively considering both attribute and structure information. The connected relationships between different nodes could be reflected by \mathbf{S} . Therefore, we utilize \mathbf{S} to refine the structure in augmented view with Hadamard product:

$$\mathbf{Aug}_S = \mathbf{Aug}_S \odot \mathbf{S}. \quad (11)$$

Pseudo Labels Matrix Refinement To further improve the reliability of the learned structure matrix, we extract the reliable clustering information to construct the matrix to further refine the structure in augmented view. Concretely, we utilize the top τ high-confidence pseudo labels \mathbf{p} to construct the matrix as follows:

$$\mathbf{Z}_{ij} = \begin{cases} 1 & \mathbf{p}_i = \mathbf{p}_j, \\ 0 & \mathbf{p}_i \neq \mathbf{p}_j. \end{cases} \quad (12)$$

where \mathbf{Z}_{ij} denotes the category relation between i -th and j -th samples. In detail, when $\mathbf{Z}_{ij} = 1$, two samples have the same pseudo label. While $\mathbf{Z}_{ij} = 0$ implies two samples have the different pseudo labels. The pseudo label matrix is constructed by the high-confidence category information. Therefore, the adjacency relation in the graph could be well reflected, leading to optimize the structure of the learned structure in the augmented view. The pseudo labels matrix refines the learned structure with Hadamard product as:

$$\mathbf{Aug}_S = \mathbf{Aug}_S \odot \mathbf{Z}. \quad (13)$$

In summary, in this subsection, we propose two strategies to refine the structure of the augmented view. By this setting, the reliability of the learned structure \mathbf{Aug}_S is improved, and the important topological could be preserved. Moreover, we introduce the detailed implementation of our method with PyTorch-style pseudo codes in Algorithm 2.

3.4 Loss Function

The proposed GCC-LDA framework follows the common contrastive learning paradigm, where the model maximize the agreement of the cross-view [61], [66], [67], [68], [69]. In detail, GCC-LDA jointly optimizes two loss functions, including the learnable augmentation loss \mathcal{L}_a and the contrastive loss \mathcal{L}_c .

To be specific, \mathcal{L}_a is the Mean Squared Error (MSE) loss between the original graph and the learnable graph, which can be formulated as:

$$\mathcal{L}_a = -(\|\mathbf{A} - \mathbf{Aug}_S\|_2^2 + \|\mathbf{X} - \mathbf{Aug}_X\|_2^2), \quad (14)$$

where \mathbf{A} , \mathbf{Aug}_S and \mathbf{X} , \mathbf{Aug}_X are the original and the learned structure, the original and the learned attribute respectively.

In GCC-LDA, we utilize the normalized temperature-scaled cross-entropy loss (NT-Xent) to pull close the positive samples, while pushing the negative samples away. The contrastive loss \mathcal{L}_c is defined as:

$$\begin{aligned}l_{i,j} &= -\log \frac{\exp(\text{sim}(\mathbf{E}_i^{v_1}, \mathbf{E}_i^{v_2})/tmp)}{\sum_{k=1, k \neq i}^N \exp(\text{sim}(\mathbf{E}_i^{v_1}, \mathbf{E}_k^{v_2})/tmp)}, \\ \mathcal{L}_c &= \frac{1}{2N} \sum_{k=1}^N [l(2k-1, 2k) + l(2k, 2k-1)],\end{aligned}\quad (15)$$

where tmp is a temperature parameter. $\text{sim}(\cdot)$ denotes the function to calculate the similarity, e.g. inner product.

The total loss of GCC-LDA is calculated as:

$$\mathcal{L} = \mathcal{L}_a + \alpha \mathcal{L}_c, \quad (16)$$

where α is the trade-off between \mathcal{L}_a and \mathcal{L}_c . The first term in Eq.(16) encourages the network to generate the augmented view with distinct semantics to ensure the diversity in input space, while the second term is the contrastive paradigm to learn the consistency of two views in latent space. The discriminative capacity of the network could be improved by minimizing the total loss function in an adversarial manner. The detailed learning process of GCC-LDA is shown in Algorithm 1.

The memory cost of \mathcal{L} is acceptable. The detailed experiments are shown in section 4.3. Besides, we design a two-stage training strategy during the overall training procedure. To be specific, the discriminative capacity of the network is improved by the first training stage. Then, in the second stage, we refine the learned structure \mathbf{Aug}_S in the augmented view with the more reliable similarity matrix and the pseudo labels matrix.

4 EXPERIMENT

4.1 Experimental Setup

Benchmark Datasets The experiments are implemented on four widely-used benchmark datasets, including CORA [43], BAT [76], EAT [76], AMAP [18], CITESEER¹, and UAT [76]. The summarized information is shown in Table 3.

Training Details The experiments are conducted on the PyTorch deep learning platform with the Intel Core i7-7820x CPU, one NVIDIA GeForce RTX 2080Ti GPU, 64GB RAM. The max training epoch number is set to 400. For fairness, we conduct ten runs for all methods. For the baselines, we adopt their source with original settings and reproduce the results.

¹ <http://citeseerx.ist.psu.edu/index>

Table 2: Clustering performance on CORA and BAT datasets (mean \pm std). Best results are **bold** values and the second best values are underlined.

Methods			CORA				BAT			
			ACC (%)	NMI (%)	ARI (%)	F1 (%)	ACC (%)	NMI (%)	ARI (%)	F1 (%)
DEC	[70]	ICML 2016	46.50 \pm 0.26	23.54 \pm 0.34	15.13 \pm 0.42	39.23 \pm 0.17	42.09 \pm 2.21	14.10 \pm 1.99	07.99 \pm 1.21	42.63 \pm 2.35
DCN	[71]	ICML 2017	49.38 \pm 0.91	25.65 \pm 0.65	21.63 \pm 0.58	43.71 \pm 1.05	47.79 \pm 3.95	18.03 \pm 7.73	13.75 \pm 6.05	46.80 \pm 3.44
MGAE	[19]	CIKM 2019	43.38 \pm 2.11	28.78 \pm 2.97	16.43 \pm 1.65	33.48 \pm 3.05	53.59 \pm 2.04	30.59 \pm 2.06	24.15 \pm 1.70	50.83 \pm 3.23
DAEGC	[36]	IJCAI 2019	70.43 \pm 0.36	52.89 \pm 0.69	49.63 \pm 0.43	68.27 \pm 0.57	52.67 \pm 0.00	21.43 \pm 0.35	18.18 \pm 0.29	52.23 \pm 0.03
ARGA	[20]	TCYB 2019	71.04 \pm 0.25	51.06 \pm 0.52	47.71 \pm 0.33	69.27 \pm 0.39	67.86 \pm 0.80	<u>49.09\pm0.54</u>	<u>42.02\pm1.21</u>	67.02 \pm 1.15
SDCN	[17]	WWW 2020	35.60 \pm 2.83	14.28 \pm 1.91	07.78 \pm 3.24	24.37 \pm 1.04	53.05 \pm 4.63	25.74 \pm 5.71	21.04 \pm 4.97	46.45 \pm 5.90
AdaGAE	[72]	TPAMI 2021	50.06 \pm 1.58	32.19 \pm 1.34	28.25 \pm 0.98	53.53 \pm 1.24	43.51 \pm 0.48	15.84 \pm 0.78	07.80 \pm 0.41	43.15 \pm 0.77
AGE	[43]	SIGKDD 2020	<u>73.50\pm1.83</u>	<u>57.58\pm1.42</u>	50.10 \pm 2.14	<u>69.28\pm1.59</u>	56.68 \pm 0.76	36.04 \pm 1.54	26.59 \pm 1.83	55.07 \pm 0.80
MVGRL	[22]	ICML 2020	70.47 \pm 3.70	55.57 \pm 1.54	48.70 \pm 3.94	67.15 \pm 1.86	37.56 \pm 0.32	29.33 \pm 0.70	13.45 \pm 0.03	29.64 \pm 0.49
DFCN	[21]	AAAI 2021	36.33 \pm 0.49	19.36 \pm 0.87	04.67 \pm 2.10	26.16 \pm 0.50	55.73 \pm 0.06	48.77 \pm 0.51	37.76 \pm 0.23	50.90 \pm 0.12
GDCL	[23]	IJCAI 2021	70.83 \pm 0.47	56.60 \pm 0.36	48.05 \pm 0.72	52.88 \pm 0.97	45.42 \pm 0.54	31.70 \pm 0.42	19.33 \pm 0.57	39.94 \pm 0.57
DCRN	[18]	AAAI 2022	61.93 \pm 0.47	45.13 \pm 1.57	33.15 \pm 0.14	49.50 \pm 0.42	<u>67.94\pm1.45</u>	47.23 \pm 0.74	39.76 \pm 0.87	<u>67.40\pm0.35</u>
AGC-DRR	[73]	IJCAI 2022	40.62 \pm 0.55	18.74 \pm 0.73	14.80 \pm 1.64	31.23 \pm 0.57	47.79 \pm 0.02	19.91 \pm 0.24	14.59 \pm 0.13	42.33 \pm 0.51
SLAPS	[74]	NeurIPS 2021	64.21 \pm 0.12	41.16 \pm 1.24	35.96 \pm 0.65	63.72 \pm 0.26	41.22 \pm 1.25	17.05 \pm 0.87	06.86 \pm 2.14	37.64 \pm 0.57
SUBLIME	[75]	WWW 2022	71.14 \pm 0.74	53.88 \pm 1.02	<u>50.15\pm0.14</u>	63.11 \pm 0.58	45.04 \pm 0.19	22.03 \pm 0.48	14.45 \pm 0.87	44.00 \pm 0.62
GCA	[61]	WWW 2021	53.62 \pm 0.73	46.87 \pm 0.65	30.32 \pm 0.98	45.73 \pm 0.47	54.89 \pm 0.34	38.88 \pm 0.23	26.69 \pm 2.85	53.71 \pm 0.34
AFGRL	[60]	AAAI 2022	26.25 \pm 1.24	12.36 \pm 1.54	14.32 \pm 1.87	30.20 \pm 1.15	50.92 \pm 0.44	27.55 \pm 0.62	21.89 \pm 0.74	46.53 \pm 0.57
AutoSSL	[63]	ICLR 2022	63.81 \pm 0.57	47.62 \pm 0.45	38.92 \pm 0.77	56.42 \pm 0.21	42.43 \pm 0.47	17.84 \pm 0.98	13.11 \pm 0.81	34.84 \pm 0.15
GCC-LDA	Ours		74.91\pm1.78	58.16\pm0.83	53.82\pm2.25	73.33\pm1.86	75.50\pm0.87	50.58\pm0.90	47.45\pm1.53	75.40\pm0.88

Algorithm 1 GCC-LDA

Input: The input graph $\mathbf{G} = \{\mathbf{X}, \mathbf{A}\}$; The iteration number I ; num: epoch to begin second training stage; Hyper-parameters τ, α .

Output: The clustering result \mathbf{R} .

```

1: for  $i = 1$  to  $I$  do
2:   Obtain the learned structure matrix  $\mathbf{Aug}_S$  and attribute matrix  $\mathbf{Aug}_X$  with our augmentors.
3:   Encode the node with the network  $\mathcal{F}(\cdot)$  to obtain the node embeddings  $\mathbf{E}^{v_1}$  and  $\mathbf{E}^{v_2}$  with Eq. (7).
4:   Fuse  $\mathbf{E}^{v_1}$  and  $\mathbf{E}^{v_2}$  to obtain  $\mathbf{E}$  with Eq. (9).
5:   Perform K-means on  $\mathbf{E}$  to obtain the clustering result.
6:   Calculate the similarity matrix of  $\mathbf{E}^{v_1}$  and  $\mathbf{E}^{v_2}$ .
7:   Obtain high-confidence pseudo label matrix.
8:   if  $i > num$  then
9:     Refine the learned structure matrix  $\mathbf{Aug}_S$  with Eq.(11) and Eq. (13).
10:  end if
11:  Calculate the learnable augmentation loss  $\mathcal{L}_a$  with Eq. (14).
12:  Calculate the contrastive loss  $\mathcal{L}_c$  with Eq. (15).
13:  Update the whole network by minimizing  $\mathcal{L}$  in Eq. (16).
14: end for
15: Perform K-means on  $\mathbf{E}$  to obtain the final clustering result  $\mathbf{R}$ .
16: return  $\mathbf{R}$ 

```

Evaluation Metrics The clustering performance is evaluated by four metrics including Accuracy (ACC), Normalized Mutual Information (NMI), Average Rand Index (ARI), and macro F1-

Table 3: Dataset information.

Dataset	Type	Sample	Dimension	Edge	Class
CORA	Graph	2708	1433	5429	7
AMAP	Graph	7650	745	119081	8
CITeseer	Graph	3327	3703	4732	6
UAT	Graph	1190	239	13599	4
BAT	Graph	131	81	1038	4
EAT	Graph	399	203	5994	4

score (F1) [77], [78], [79].

Parameter Setting In our model, the learning rate is set to 1e-3 for UAT, 1e-4 for CORA/CITeseer, 1e-5 for AMAP/BAT, and 1e-7 for EAT, respectively. The threshold τ is set to 95% for all datasets. The epoch to begin second training stage num is set to 200. The trade-off α is set to 0.5.

4.2 Performance Comparison

In this subsection, to verify the superiority of GCC-LDA, we compare the clustering performance of our proposed algorithm with 18 baselines on four datasets with four metrics. We divide these methods into four categories, i.e. classical deep clustering methods

Table 4: Clustering performance on AMAP and EAT datasets (mean \pm std). Best results are **bold** values and the second best values are underlined.

Methods			AMAP				EAT			
			ACC (%)	NMI (%)	ARI (%)	F1 (%)	ACC (%)	NMI (%)	ARI (%)	F1 (%)
DEC	[70]	ICML 2016	47.22 \pm 0.08	37.35 \pm 0.05	18.59 \pm 0.04	46.71 \pm 0.12	36.47 \pm 1.60	04.96 \pm 1.74	03.60 \pm 1.87	34.84 \pm 1.28
DCN	[71]	ICML 2017	48.25 \pm 0.08	38.76 \pm 0.30	20.80 \pm 0.47	47.87 \pm 0.20	38.85 \pm 2.32	06.92 \pm 2.80	05.11 \pm 2.65	38.75 \pm 2.25
MGAE	[19]	CIKM 2019	71.57 \pm 2.48	62.13 \pm 2.79	48.82 \pm 4.57	68.08 \pm 1.76	44.61 \pm 2.10	15.60 \pm 2.30	13.40 \pm 1.26	43.08 \pm 3.26
DAEGC	[36]	IJCAI 2019	75.96 \pm 0.23	65.25 \pm 0.45	58.12 \pm 0.24	69.87 \pm 0.54	36.89 \pm 0.15	05.57 \pm 0.06	05.03 \pm 0.08	34.72 \pm 0.16
ARGA	[20]	TCYB 2019	69.28 \pm 2.30	58.36 \pm 2.76	44.18 \pm 4.41	64.30 \pm 1.95	<u>52.13\pm0.00</u>	22.48 \pm 1.21	17.29 \pm 0.50	52.75 \pm 0.07
SDCN	[17]	WWW 2020	53.44 \pm 0.81	44.85 \pm 0.83	31.21 \pm 1.23	50.66 \pm 1.49	39.07 \pm 1.51	08.83 \pm 2.54	06.31 \pm 1.95	33.42 \pm 3.10
AdaGAE	[72]	TPAMI 2021	67.70 \pm 0.54	55.96 \pm 0.87	46.20 \pm 0.45	62.95 \pm 0.74	32.83 \pm 1.24	04.36 \pm 1.87	02.47 \pm 0.54	32.39 \pm 0.47
AGE	[43]	SIGKDD 2020	75.98 \pm 0.68	65.38 \pm 0.61	55.89 \pm 1.34	<u>71.74\pm0.93</u>	47.26 \pm 0.32	23.74 \pm 0.90	16.57 \pm 0.46	45.54 \pm 0.40
MVGRL	[22]	ICML 2020	41.07 \pm 3.12	30.28 \pm 3.94	18.77 \pm 2.34	32.88 \pm 5.50	32.88 \pm 0.71	11.72 \pm 1.08	04.68 \pm 1.30	25.35 \pm 0.75
DFCN	[21]	AAAI 2021	76.82 \pm 0.23	66.23 \pm 1.21	58.28 \pm 0.74	71.25 \pm 0.31	49.37 \pm 0.19	<u>32.90\pm0.41</u>	23.25 \pm 0.18	42.95 \pm 0.04
GDCL	[23]	IJCAI 2021	43.75 \pm 0.78	37.32 \pm 0.28	21.57 \pm 0.51	38.37 \pm 0.29	33.46 \pm 0.18	13.22 \pm 0.33	04.31 \pm 0.29	25.02 \pm 0.21
DCRN	[18]	AAAI 2022	OOM	OOM	OOM	OOM	50.88 \pm 0.55	22.01 \pm 1.23	18.13 \pm 0.85	47.06 \pm 0.66
AGC-DRR	[73]	IJCAI 2022	<u>76.81\pm1.45</u>	<u>66.54\pm1.24</u>	60.15\pm1.56	71.03 \pm 0.64	37.37 \pm 0.11	07.00 \pm 0.85	04.88 \pm 0.91	35.20 \pm 0.17
SLAPS	[74]	NeurIPS 2021	60.09 \pm 1.14	51.15 \pm 0.87	42.87 \pm 0.75	47.73 \pm 0.98	48.62 \pm 1.65	28.33 \pm 2.56	<u>24.59\pm0.58</u>	40.42 \pm 1.44
SUBLIME	[75]	WWW 2022	27.22 \pm 1.56	06.37 \pm 1.89	05.36 \pm 2.14	15.97 \pm 1.53	38.80 \pm 0.35	14.96 \pm 0.75	10.29 \pm 0.88	32.31 \pm 0.97
GCA	[61]	WWW 2021	56.81 \pm 1.44	48.38 \pm 2.38	26.85 \pm 0.44	53.59 \pm 0.57	48.51 \pm 1.55	28.36 \pm 1.23	19.61 \pm 1.25	<u>48.22\pm0.33</u>
AFGRL	[60]	AAAI 2022	75.51 \pm 0.77	64.05 \pm 0.15	54.45 \pm 0.48	69.99 \pm 0.34	37.42 \pm 1.24	11.44 \pm 1.41	06.57 \pm 1.73	30.53 \pm 1.47
AutoSSL	[63]	ICLR 2022	54.55 \pm 0.97	48.56 \pm 0.71	26.87 \pm 0.34	54.47 \pm 0.83	31.33 \pm 0.52	17.63 \pm 0.85	12.13 \pm 0.67	21.82 \pm 0.98
GCC-LDA	Ours		77.24\pm0.87	67.12\pm0.92	<u>58.14\pm0.82</u>	73.02\pm2.34	57.22\pm0.73	33.47\pm0.34	26.21\pm0.81	57.53\pm0.67

(DEC [70], DCN [71], MGAE [80], DAEGC [36], ARGA [20], SDCN [17], AdaGAE [72]), contrastive deep graph clustering methods (AGE [43], MVGRL [22], DFCN [21], GDCL [23], DCRN [18], AGC-DRR [73]), graph structure learning methods (SLAPS [74], SUBLIME [75]), and graph augmentation methods (GCA [61], AFGRL [60], AutoSSL [63]).

Here, we adopt the attention structure augmentor and the MLP attribute augmentor to generate the augmented view in a learnable way. From the results in Table.2, Table.5 and Table.4, we observe and analyze as follows: 1) GCC-LDA obtains better performance compared with classical deep graph clustering methods. The reason is that they rarely consider the topological information in the graph. 2) Contrastive deep graph clustering methods achieve sub-optimal performance compared with ours. We conjecture that the discriminative capacity of our GCC-LDA is improved with the learnable augmentation and the optimization strategies. 3) The classical graph augmentation methods achieve the unsatisfied clustering performance. This is because they merely consider the learnable of the structure, while neglecting the attribute. Moreover, almost of those methods can not optimize with the downstream tasks. 4) It could be observed that the graph structure learning methods are not comparable with ours. We analyze the reason is that those methods refine the structure with the unreliable strategy at the beginning of the training. In summary, our method outperforms most of other algorithms on four datasets with four metrics. Taking the result on CORA dataset for example, GCC-LDA exceeds the runner-up by 1.41%, 0.58%, 3.72%, 4.05% with

respect to ACC, NMI, ARI, and F1.

4.3 Time Cost and Memory Cost

In this subsection, we implement time and memory cost experiments to demonstrate the effectiveness of the proposed GCC-LDA.

Specifically, we test the training time of GCC-LDA with five baselines on four datasets. For fairness, we train all algorithms with 400 epochs. From the results in Table 7, we observe that the training time of GCC-LDA is comparable with other eight algorithms. The reason we analyze is as follows: instead of using GCN as the encoder network, we adopt graph filter to smooth the feature. This operation effectively reduces time consumption.

Moreover, we conduct experiments to test GPU memory costs of our proposed GCC-LDA with five methods (i.e., DAEGC [36], SDCN [17], AGE [43], MVGRL [22], SCAGC [44]) on six datasets. From the results in Fig. 3, we observe that the memory costs of our GCC-LDA are also comparable with other algorithms.

4.4 Ablation Studies

In this section, we first conduct ablation studies to verify the effectiveness of the proposed modules, and then we analyze the robustness of GCC-LDA to the hyper-parameters. Last, we conduct experiments to verify the effectiveness of our proposed loss function.

Table 5: Clustering performance on UAT and CITESEER datasets (mean \pm std). Best results are **bold** values and the second best values are underlined.

Method			UAT				CITESEER			
			ACC (%)	NMI (%)	ARI (%)	F1 (%)	ACC (%)	NMI (%)	ARI (%)	F1 (%)
DEC	[70]	ICML 2016	45.61 \pm 1.84	16.63 \pm 2.39	13.14 \pm 1.97	44.22 \pm 1.51	55.89 \pm 0.20	28.34 \pm 0.30	28.12 \pm 0.36	52.62 \pm 0.17
DCN	[71]	ICML 2017	46.82 \pm 1.14	17.18 \pm 1.60	13.59 \pm 2.02	45.66 \pm 1.49	57.08 \pm 0.13	27.64 \pm 0.08	29.31 \pm 0.14	53.80 \pm 0.11
MGAE	[19]	CIKM 2019	48.97 \pm 1.52	20.69 \pm 0.98	18.33 \pm 1.79	47.95 \pm 1.52	61.35 \pm 0.80	34.63 \pm 0.65	33.55 \pm 1.18	57.36 \pm 0.82
DAEGC	[36]	IJCAI 2019	52.29 \pm 0.49	21.33 \pm 0.44	20.50 \pm 0.51	<u>50.33\pm0.64</u>	64.54 \pm 1.39	36.41 \pm 0.86	37.78 \pm 1.24	62.20 \pm 1.32
ARGA	[20]	TCYB 2019	49.31 \pm 0.15	<u>25.44\pm0.31</u>	16.57 \pm 0.31	50.26 \pm 0.16	61.07 \pm 0.49	34.40 \pm 0.71	34.32 \pm 0.70	58.23 \pm 0.31
SDCN	[17]	WWW 2020	52.25 \pm 1.91	21.61 \pm 1.26	21.63 \pm 1.49	45.59 \pm 3.54	65.96 \pm 0.31	38.71 \pm 0.32	40.17 \pm 0.43	63.62 \pm 0.24
AdaGAE	[72]	TPAMI 2021	52.10 \pm 0.87	26.02 \pm 0.71	24.47\pm0.13	43.44 \pm 0.85	54.01 \pm 1.11	27.79 \pm 0.47	24.19 \pm 0.85	51.11 \pm 0.64
AGE	[43]	SIGKDD 2020	<u>52.37\pm0.42</u>	23.64 \pm 0.66	20.39 \pm 0.70	50.15 \pm 0.73	69.73 \pm 0.24	44.93\pm0.53	45.31 \pm 0.41	64.45 \pm 0.27
MVGRG	[22]	ICML 2020	44.16 \pm 1.38	21.53 \pm 0.94	17.12 \pm 1.46	39.44 \pm 2.19	62.83 \pm 1.59	40.69 \pm 0.93	34.18 \pm 1.73	59.54 \pm 2.17
DFCN	[21]	AAAI 2021	33.61 \pm 0.09	26.49\pm0.41	11.87 \pm 0.23	25.79 \pm 0.29	69.50 \pm 0.20	43.90 \pm 0.20	<u>45.50\pm0.30</u>	64.30 \pm 0.20
GDCL	[23]	IJCAI 2021	48.70 \pm 0.06	25.10 \pm 0.01	21.76 \pm 0.01	45.69 \pm 0.08	66.39 \pm 0.65	39.52 \pm 0.38	41.07 \pm 0.96	61.12 \pm 0.70
DCRN	[18]	AAAI 2022	49.92 \pm 1.25	24.09 \pm 0.53	17.17 \pm 0.69	44.81 \pm 0.87	<u>69.86\pm0.18</u>	<u>44.86\pm0.35</u>	45.64\pm0.30	<u>64.83\pm0.21</u>
AGC-DRR	[73]	IJCAI 2022	42.64 \pm 0.31	11.15 \pm 0.24	09.50 \pm 0.25	35.18 \pm 0.32	68.32 \pm 1.83	43.28 \pm 1.41	45.34 \pm 2.33	64.82 \pm 1.60
SLAPS	[74]	NIPS 2021	49.77 \pm 1.24	12.86 \pm 0.65	17.36 \pm 0.98	10.56 \pm 1.34	64.14 \pm 0.65	39.08 \pm 0.25	39.27 \pm 0.78	61.00 \pm 0.15
SUBLIME	[75]	WWW 2022	48.74 \pm 0.54	21.85 \pm 0.62	19.51 \pm 0.45	46.19 \pm 0.87	68.25 \pm 1.21	43.15 \pm 0.14	44.21 \pm 0.54	63.12 \pm 0.42
GCA	[61]	WWW 2021	39.39 \pm 1.46	24.05 \pm 0.25	14.37 \pm 0.19	35.72 \pm 0.28	60.45 \pm 1.03	36.15 \pm 0.78	35.20 \pm 0.96	56.42 \pm 0.94
AFGRL	[60]	AAAI 2022	41.50 \pm 0.25	17.33 \pm 0.54	13.62 \pm 0.57	36.52 \pm 0.89	31.45 \pm 0.54	15.17 \pm 0.47	14.32 \pm 0.78	30.20 \pm 0.71
AutoSSL	[63]	ICLR 2022	42.52 \pm 0.64	17.86 \pm 0.22	13.13 \pm 0.71	34.94 \pm 0.87	66.76 \pm 0.67	40.67 \pm 0.84	38.73 \pm 0.55	58.22 \pm 0.68
GCC-LDA	Ours		54.76\pm1.42	25.23 \pm 0.96	<u>22.44\pm1.69</u>	53.61\pm2.61	70.12\pm0.36	43.56 \pm 0.35	44.85 \pm 0.69	65.01\pm0.39

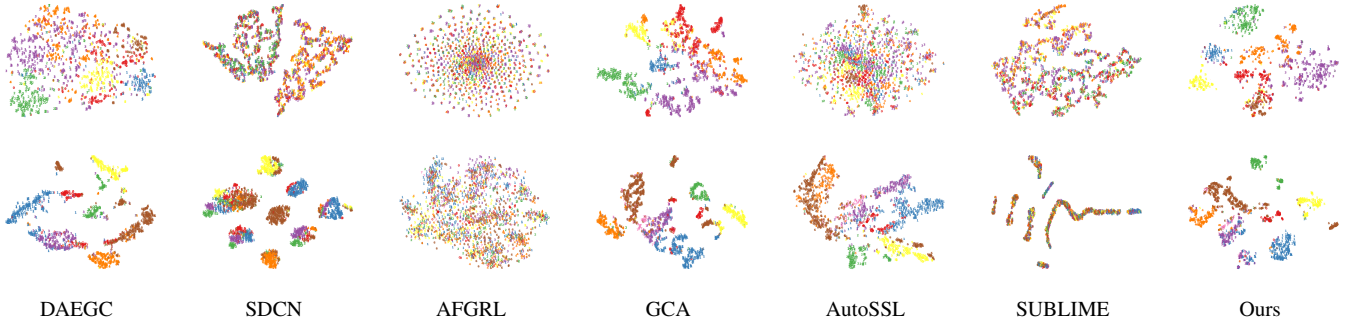


Figure 2: 2D t -SNE visualization of seven methods on two benchmark datasets. The first row and second row corresponds to CORA and AMAP dataset, respectively.

4.4.1 Effectiveness of the Structure and Attribute Augmentor

To verify the effect of the proposed structure and attribute augmentor, we conduct extensive experiments as shown in Table 6. Here, we adopt “(w/o) Aug_X ”, “(w/o) Aug_S ” and “(w/o) Aug_X & Aug_S ” to represent the reduced models by removing the structure augmentor, the attribute augmentor, and both, respectively. From the observations, it is apparent that the performance will decrease without any of our proposed augmentors, revealing that both augmentors make essential contributions to boosting the performance. Taking the result on the CORA dataset for example, the model performance is improved substantially by utilizing the attribute

augmentor.

4.4.2 Effectiveness of the Similarity and Pseudo-label Matrix Optimization

In this subsection, we implement experiments to verify the effectiveness of our optimization strategies, i.e. Similarity Matrix Optimization and Pseudo-label Matrix Optimization. Here, we adopt the model without any optimization strategy as the baseline. For simplicity, we denote “NP+NS”, “S”, “P”, and “P+S” as the baseline, baseline with similarity matrix optimization, baseline with pseudo-label matrix optimization, and ours, respectively. From the results in Fig. 4, we observe that the performance of

Table 6: Ablation studies over the learnable graph augmentation module of GCC-LDA on four datasets. “(w/o) Aug_X ”, “(w/o) Aug_S ” and “(w/o) Aug_X & Aug_S ” to represent the reduced models by removing the structure augmentor, the attribute augmentor, and both, respectively. Additionally, our algorithm is compared with four classic data augmentations.

Dataset	Metric	(w/o) Aug_X	(w/o) Aug_S	(w/o) Aug_X & Aug_S	Mask Feature	Drop Edges	Add Edges	Diffusion	Ours
CORA	ACC	65.60±4.95	71.92±1.32	62.16±2.57	70.60±0.91	60.29±2.42	68.02±1.93	72.68±1.00	74.91±1.78
	NMI	48.81±3.95	53.82±1.99	40.84±1.45	53.99±1.48	48.40±1.91	50.78±1.93	55.80±1.22	58.16±0.83
	ARI	42.42±5.09	49.20±1.56	34.84±2.82	47.80±1.09	39.78±2.21	43.56±1.83	50.45±1.24	53.82±2.25
	F1	60.86±8.35	69.82±0.88	60.46±3.10	69.39±0.85	55.40±4.64	66.93±1.96	69.11±0.78	73.33±1.86
AMAP	ACC	73.18±4.67	73.14±1.10	68.32±0.98	72.73±0.41	64.22±4.15	74.51±0.16	72.99±0.53	77.24±0.87
	NMI	61.27±5.13	60.99±0.75	53.76±1.12	61.99±0.59	53.07±3.57	62.94±0.28	61.57±0.92	67.12±0.92
	ARI	51.89±6.11	52.27±1.72	44.50±1.28	49.98±0.83	46.07±3.58	53.45±0.32	50.64±0.67	58.14±0.82
	F1	69.19±4.57	68.73±1.39	63.58±0.93	68.36±0.85	56.14±5.21	69.16±0.14	68.16±0.57	73.02±2.34
BAT	ACC	69.01±2.58	70.84±2.64	64.43±2.35	58.85±3.14	53.28±2.60	66.03±3.19	56.95±3.63	75.50±0.87
	NMI	46.52±1.00	47.96±2.04	40.98±2.30	38.04±2.80	28.44±2.01	41.05±3.20	37.79±4.76	50.58±0.90
	ARI	42.16±1.43	42.97±2.08	35.19±2.96	25.67±4.52	20.86±2.67	36.03±4.28	29.43±3.67	47.45±1.53
	F1	67.05±4.28	70.03±3.71	63.08±3.08	57.94±3.94	52.27±3.00	65.09±3.15	49.84±4.73	75.40±0.88
EAT	ACC	56.42±1.57	55.31±0.88	38.80±1.67	50.13±2.11	47.19±1.81	40.03±5.50	45.56±1.86	57.22±0.73
	NMI	33.11±1.34	32.65±1.02	12.06±2.35	25.74±2.54	28.25±4.64	09.01±7.18	21.12±3.12	33.47±0.34
	ARI	26.66±0.95	25.70±0.86	07.72±2.55	18.46±2.48	22.37±4.43	07.72±6.23	16.28±4.00	26.21±0.81
	F1	56.36±1.99	54.51±2.79	31.53±2.62	48.40±4.36	44.39±2.37	38.57±5.36	36.22±2.63	57.53±0.67
CITSEER	ACC	48.54±0.54	57.86±0.67	39.25±0.85	63.62±1.10	66.00±1.47	64.16±1.06	65.74±0.56	70.12±0.36
	NMI	20.23±0.23	30.73±0.84	27.67±0.41	39.13±1.17	39.46±1.44	39.35±1.13	40.98±0.57	43.56±0.35
	ARI	13.34±0.66	27.13±0.45	12.57±0.72	37.09±1.73	38.66±2.24	37.78±1.43	39.66±0.91	44.85±0.69
	F1	43.50±0.42	54.73±0.58	30.40±0.28	60.36±0.85	58.50±1.24	60.39±1.01	62.00±0.81	65.01±0.39
UAT	ACC	47.61±1.52	49.83±1.17	45.65±0.66	47.09±2.19	53.09±0.71	50.47±1.31	52.39±2.00	54.76±1.42
	NMI	21.66±1.42	25.46±0.62	18.50±1.25	16.79±2.90	22.61±0.67	23.20±1.43	23.30±1.26	25.23±0.96
	ARI	17.71±1.90	21.62±1.06	14.46±1.72	11.82±3.19	21.00±1.58	14.64±2.76	22.17±2.43	19.44±1.69
	F1	43.01±2.30	47.69±1.64	45.58±0.80	45.04±2.37	51.32±0.86	50.26±2.45	48.81±2.62	53.61±2.61

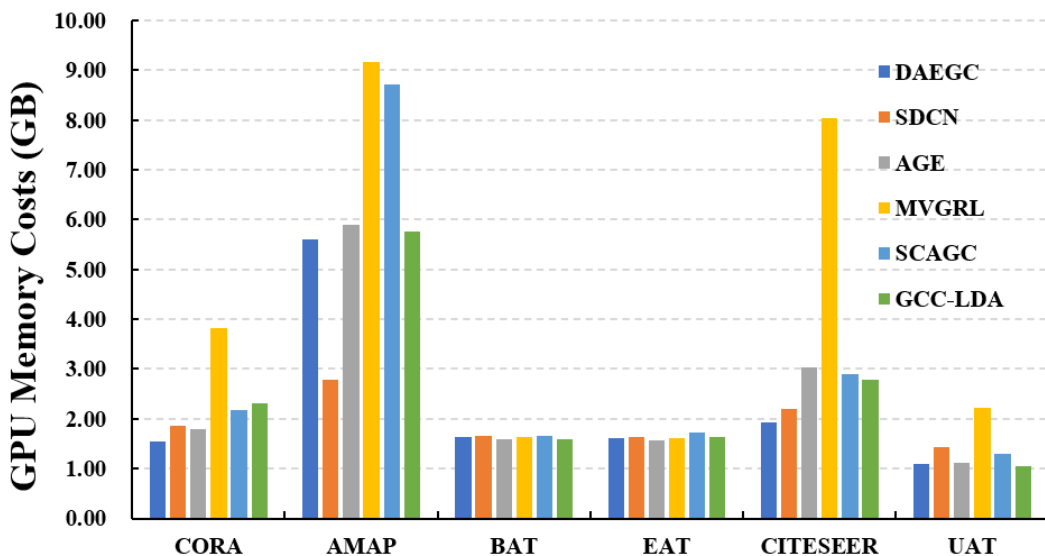


Figure 3: GPU memory costs on six datasets with five methods.

Table 7: Training Time Comparison on six datasets with nine methods. The algorithms are measured by seconds. The Avg. represents the average time cost on six dataset. Moreover, OOM denotes Out-Of-Memory during training process.

Dataset	Classical Methods					Contrastive Methods				
	DEC [70]	DCN [71]	MGAE [19]	DAEGC [36]	SDCN [17]	AGE [43]	MVGRL [22]	MCGC [81]	SCAGC [44]	GCC-LDA
	ICML 2016	ICML 2017	SIGKDD 2019	IJCAI 2019	WWW 2020	SIGKDD 2020	ICML 2020	NeurIPS 2021	TMM 2022	Ours
CORA	91.13	47.31	7.38	12.97	11.32	46.65	14.72	118.07	54.08	10.06
BAT	21.37	7.46	3.83	4.79	11.50	2.49	3.19	2.28	93.79	1.89
EAT	26.99	9.56	4.64	5.14	12.12	3.86	3.32	2.87	47.79	2.21
AMAP	264.20	94.48	18.64	39.62	19.28	377.49	131.38	OOM	150.54	83.26
CITSEER	223.95	74.49	6.69	14.70	11.00	70.76	18.31	126.06	50.00	17.24
UAT	42.30	29.57	4.75	6.44	10.64	8.95	4.27	23.10	64.70	4.15
Avg.	111.66	43.85	7.66	13.94	12.64	85.01	29.20	–	76.82	19.80

Algorithm 2 PyTorch-style Pseudo Code of Our Method.

```

# X: Original Attribute, A: Original Structure
# AG: Attribute Augmentor
# SG: Structure Augmentor
# P: High-confidence Pseudo Labels
# num: Epoch to begin second training stage
# sim: Similarity Function, simclr: simclr loss
# alpha: trade-off parameter
for epoch in range(epoch_num):
    # Attribute Matrix and Adjacency Matrix
    Aug_X = AG(X)
    Aug_S = SG(A)

    # Net Encoding
    E1 = F.normalization((X, A), dim=1, p=2)
    E2 = F.normalization((Gen_X, Gen_A), dim=1, p=2)
    # Clustering and High-confidence Pseudo Label
    clu_res, P = clustering((E1+E2)/2)

    # Cross-view Similarity Matrix
    M = E1 @ E2.T
    # Pseudo Label Matrix
    Q = (P==P.T).int()

    loss_c = simclr(E1, E2)
    loss = loss_c

    if epoch > num:
        # Structure Refine
        Gen_A = Aug_S * M
        Gen_A = Aug_S * Q

        loss_a = -(MSE(X, Aug_X) + MSE(A, Aug_S))
        loss = loss_c + alpha * loss_a
    # optimization
    loss.backward()
    optimizer.step()
    clu_res, _, _ = clustering((E1+E2)/2)
    return clu_res

```

the GCC-LDA will decrease when any one of the aforementioned components is dropped. Overall, expensive experiments could demonstrate the effectiveness of our optimization strategies.

4.4.3 Effectiveness of our learnable augmentation

To avoid the existing and pre-defined augmentations on graphs, we design a novel learnable augmentation method for graph clustering. In this part, we compare our view construction method with other classical graph data augmentations including mask feature [23], drop edges [44], add edges [44], and graph diffusion [56]. Concretely, in Table 6, we adopt the data augmentation as randomly dropping 20% edges (“Drop Edges”), or randomly adding 20% edges (“Add Edges”), or graph diffusion (“Diffusion”) with 0.20 teleportation rate, or randomly masking 20% features (“Mask Feature”). From the results, we observe that the performance of commonly used graph augmentations is not comparable

with ours. In summary, expensive experiments have demonstrated the effectiveness of the proposed learnable augmentation.

4.5 Hyper-parameter Analysis

4.5.1 Sensitivity Analysis of hyper-parameter α

We verify the sensitivity of α , the experimental results are shown in Fig.5. From these results, we observe that the performance will not fluctuate greatly when α is varying. This demonstrates that our GCC-LDA is insensitive to α . Moreover, we also investigate the influence of the hyper-parameter threshold τ .

4.5.2 Sensitivity Analysis of hyper-parameter τ

To investigate the influence of the hyper-parameter threshold τ , we conduct the experiments on four datasets as shown in Fig.6. From the results, we observe that the model obtains promising performance with the τ increasing. The reasons is that the pseudo labels are more reliable with high threshold.

4.6 Visualization Analysis

In this subsection, we visualize the distribution of the learned embeddings to show the superiority of GCC-LDA on CORA and AMAP datasets via t -SNE algorithm [82]. Six baselines and GCC-LDA are shown in Fig. 2, we can conclude that GCC-LDA better reveals the intrinsic clustering structure.

5 CONCLUSION

In this work, we propose a learnable augmentation method for graph contrastive clustering termed GCC-LDA. To be specific, we design a fully learnable augmentation with the Structure Augmentor and the attribute augmentor to dynamically learn the structure and attribute information, respectively. Besides, an adversarial mechanism is designed to keep cross-view consistency in the latent space while ensuring the diversity of the augmented views. Meanwhile, we propose a two-stage training strategy to obtain more reliable clustering information during the model training. Benefiting with the clustering information, we refine the learned structure with the high-confidence pseudo-label matrix. Moreover, we refine the augmented view with the cross-view sample similarity matrix to further improve the discriminative capability of the learned structure. Extensive experiments on four datasets demonstrate the effectiveness of our proposed method.

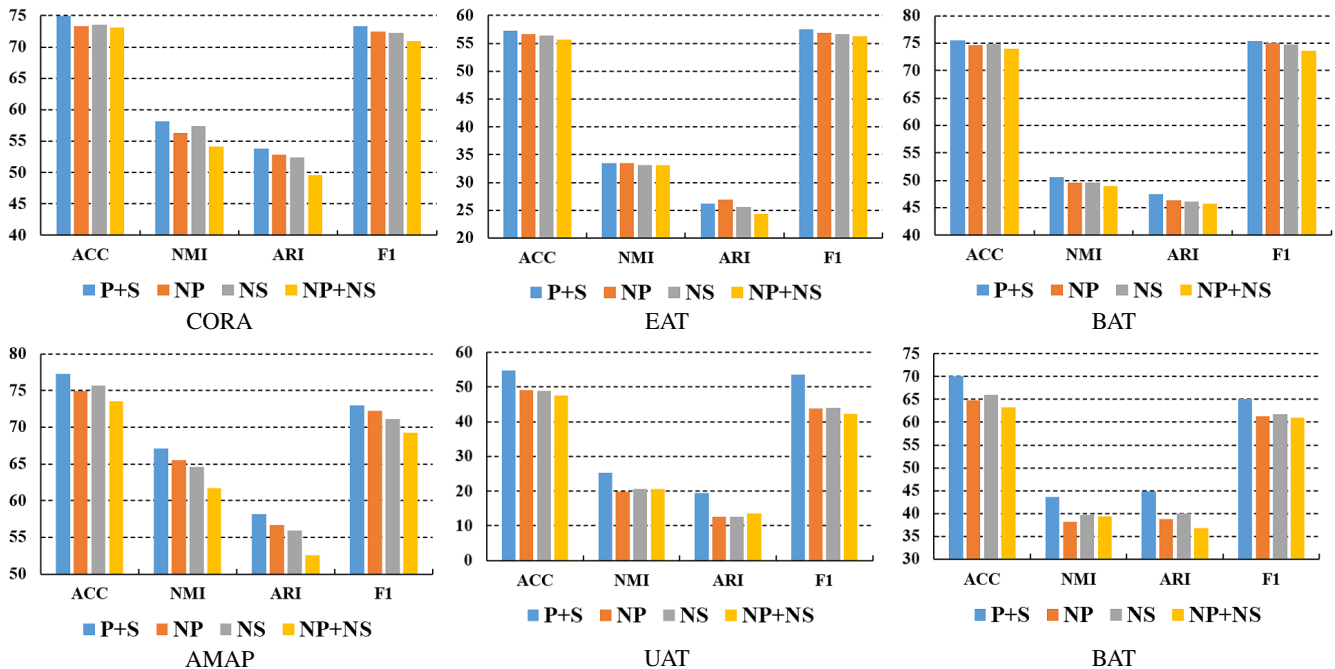


Figure 4: Ablation studies over the effectiveness of the proposed similarity matrix and pseudo labels matrix refinement strategy on six benchmark datasets. “NP+NS”, “S”, “P”, and “P+S” denotes the baseline, baseline with similarity matrix optimization, baseline with pseudo-label matrix optimization, and ours, respectively.

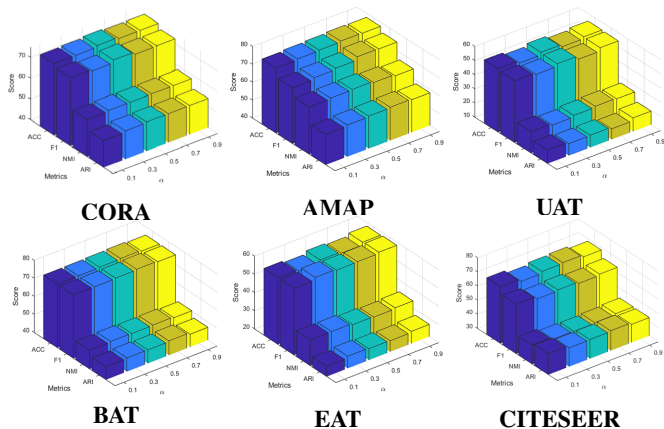


Figure 5: Sensitivity analysis of the hyper-parameter α .

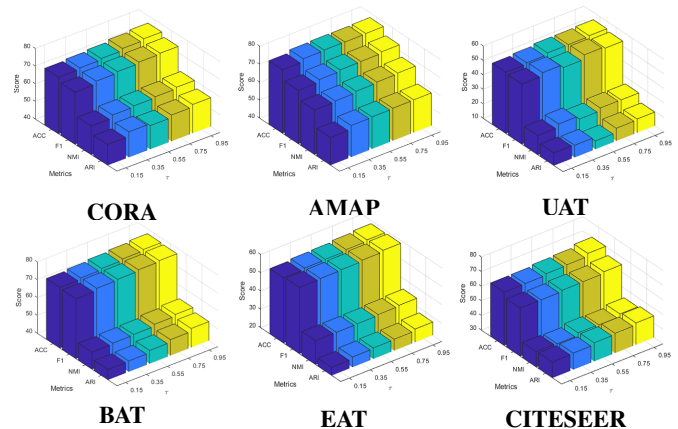


Figure 6: Sensitivity analysis of the hyper-parameter τ .

REFERENCES

- [1] X. Miao, W. Zhang, Y. Shao, B. Cui, L. Chen, C. Zhang, and J. Jiang, “Lasagne: A multi-layer graph convolutional network framework via node-aware deep architecture,” *IEEE Transactions on Knowledge and Data Engineering*, 2021.
- [2] L. Zhang, S. Wang, J. Liu, Q. Lin, X. Chang, Y. Wu, and Q. Zheng, “Mulgrn: Multi-level graph relation network for few-shot node classification,” *IEEE Transactions on Knowledge and Data Engineering*, 2022.
- [3] Y. Liu, M. Jin, S. Pan, C. Zhou, Y. Zheng, F. Xia, and P. Yu, “Graph self-supervised learning: A survey,” *IEEE Transactions on Knowledge and Data Engineering*, 2022.
- [4] X. Xu, F. Zhou, K. Zhang, and S. Liu, “Ccgl: Contrastive cascade graph learning,” *IEEE Transactions on Knowledge and Data Engineering*, 2022.
- [5] J. Xia, L. Wu, J. Chen, B. Hu, and S. Z. Li, “Simgrace: A simple framework for graph contrastive learning without data augmentation,” *arXiv preprint arXiv:2202.03104*, 2022.
- [6] T. N. Kipf and M. Welling, “Semi-supervised classification with graph convolutional networks,” in *International Conference on Learning Representations*, 2017.
- [7] P. Veličković, G. Cucurull, A. Casanova, A. Romero, P. Lio, and Y. Bengio, “Graph attention networks,” *arXiv preprint arXiv:1710.10903*, 2017.
- [8] J. Xia, L. Wu, G. Wang, J. Chen, and S. Z. Li, “Progl: Rethinking hard negative mining in graph contrastive learning,” in *International Conference on Machine Learning*. PMLR, 2022, pp. 24 332–24 346.
- [9] D. Jingcan, W. Siwei, L. Xinwang, Z. Haifang, H. Jingtao, and J. Hu, “Gadmsl: Graph anomaly detection on attributed networks via multi-scale substructure learning,” *arXiv preprint arXiv:2211.15255*, 2022.
- [10] F. Fous, A. Pirotte, J.-M. Renders, and M. Saerens, “Random-walk computation of similarities between nodes of a graph with application to collaborative recommendation,” *IEEE Transactions on knowledge and data engineering*, vol. 19, no. 3, pp. 355–369, 2007.
- [11] L. Chen, L. Wu, R. Hong, K. Zhang, and M. Wang, “Revisiting graph based collaborative filtering: A linear residual graph convolutional network approach,” in *Proceedings of the AAAI conference on artificial intelligence*, vol. 34, no. 01, 2020, pp. 27–34.
- [12] J. Xia, J. Zheng, C. Tan, G. Wang, and S. Z. Li, “Towards effective

- and generalizable fine-tuning for pre-trained molecular graph models,” *bioRxiv*, 2022.
- [13] J. Xia, Y. Zhu, Y. Du, and S. Z. Li, “Pre-training graph neural networks for molecular representations: retrospect and prospect,” in *ICML 2022 2nd AI for Science Workshop*, 2022.
- [14] D. Qin, X. Zhou, L. Chen, G. Huang, and Y. Zhang, “Dynamic connection-based social group recommendation,” *IEEE Transactions on Knowledge and Data Engineering*, vol. 32, no. 3, pp. 453–467, 2018.
- [15] W. Yu, X. Lin, J. Liu, J. Ge, W. Ou, and Z. Qin, “Self-propagation graph neural network for recommendation,” *IEEE Transactions on Knowledge and Data Engineering*, 2021.
- [16] Y. Liu, S. Yang, Y. Zhang, C. Miao, Z. Nie, and J. Zhang, “Learning hierarchical review graph representations for recommendation,” *IEEE Transactions on Knowledge and Data Engineering*, 2021.
- [17] D. Bo, X. Wang, C. Shi, M. Zhu, E. Lu, and P. Cui, “Structural deep clustering network,” in *Proceedings of The Web Conference 2020*, 2020, pp. 1400–1410.
- [18] Y. Liu, W. Tu, S. Zhou, X. Liu, L. Song, X. Yang, and E. Zhu, “Deep graph clustering via dual correlation reduction,” in *AAAI Conference on Artificial Intelligence*, 2022.
- [19] C. Wang, S. Pan, G. Long, X. Zhu, and J. Jiang, “Mgae: Marginalized graph autoencoder for graph clustering,” in *Proceedings of the 2017 ACM on Conference on Information and Knowledge Management*, 2017, pp. 889–898.
- [20] S. Pan, R. Hu, S.-f. Fung, G. Long, J. Jiang, and C. Zhang, “Learning graph embedding with adversarial training methods,” *IEEE transactions on cybernetics*, vol. 50, no. 6, pp. 2475–2487, 2019.
- [21] W. Tu, S. Zhou, X. Liu, X. Guo, Z. Cai, J. Cheng *et al.*, “Deep fusion clustering network,” *arXiv preprint arXiv:2012.09600*, 2020.
- [22] K. Hassani and A. H. Khasahmadi, “Contrastive multi-view representation learning on graphs,” in *International Conference on Machine Learning*. PMLR, 2020, pp. 4116–4126.
- [23] H. Zhao, X. Yang, Z. Wang, E. Yang, and C. Deng, “Graph debiased contrastive learning with joint representation clustering,” in *Proc. IJCAI*, 2021, pp. 3434–3440.
- [24] Y. You, T. Chen, Y. Shen, and Z. Wang, “Graph contrastive learning automated,” in *International Conference on Machine Learning*. PMLR, 2021, pp. 12 121–12 132.
- [25] S. Suresh, P. Li, C. Hao, and J. Neville, “Adversarial graph augmentation to improve graph contrastive learning,” *Advances in Neural Information Processing Systems*, vol. 34, pp. 15 920–15 933, 2021.
- [26] Y. Yin, Q. Wang, S. Huang, H. Xiong, and X. Zhang, “Autogcl: Automated graph contrastive learning via learnable view generators,” in *Proceedings of the AAAI Conference on Artificial Intelligence*, vol. 36, no. 8, 2022, pp. 8892–8900.
- [27] S. Liu, S. Wang, P. Zhang, K. Xu, X. Liu, C. Zhang, and F. Gao, “Efficient one-pass multi-view subspace clustering with consensus anchors,” in *Proceedings of the AAAI Conference on Artificial Intelligence*, vol. 36, no. 7, 2022, pp. 7576–7584.
- [28] P. Zhang, X. Liu, J. Xiong, S. Zhou, W. Zhao, E. Zhu, and Z. Cai, “Consensus one-step multi-view subspace clustering,” *IEEE Transactions on Knowledge and Data Engineering*, 2020.
- [29] M. Sun, P. Zhang, S. Wang, S. Zhou, W. Tu, X. Liu, E. Zhu, and C. Wang, “Scalable multi-view subspace clustering with unified anchors,” in *Proceedings of the 29th ACM International Conference on Multimedia*, 2021, pp. 3528–3536.
- [30] Y. Wang, X. Lin, L. Wu, W. Zhang, Q. Zhang, and X. Huang, “Robust subspace clustering for multi-view data by exploiting correlation consensus,” *IEEE Transactions on Image Processing*, vol. 24, no. 11, pp. 3939–3949, 2015.
- [31] Y. Wang, W. Zhang, L. Wu, X. Lin, M. Fang, and S. Pan, “Iterative views agreement: An iterative low-rank based structured optimization method to multi-view spectral clustering,” *arXiv preprint arXiv:1608.05560*, 2016.
- [32] Y. Wang and L. Wu, “Beyond low-rank representations: Orthogonal clustering basis reconstruction with optimized graph structure for multi-view spectral clustering,” *Neural Networks*, vol. 103, pp. 1–8, 2018.
- [33] Z. Lin, Z. Kang, L. Zhang, and L. Tian, “Multi-view attributed graph clustering,” *IEEE Transactions on Knowledge and Data Engineering*, 2021.
- [34] X. Zhang, X. Zhang, H. Liu, and X. Liu, “Multi-task multi-view clustering,” *IEEE Transactions on Knowledge and Data Engineering*, vol. 28, no. 12, pp. 3324–3338, 2016.
- [35] J. Zhang, L. Li, S. Wang, J. Liu, Y. Liu, X. Liu, and E. Zhu, “Multiple kernel clustering with dual noise minimization,” in *Proceedings of the 30th ACM International Conference on Multimedia*, 2022, pp. 3440–3450.
- [36] C. Wang, S. Pan, R. Hu, G. Long, J. Jiang, and C. Zhang, “Attributed graph clustering: A deep attentional embedding approach,” *arXiv preprint arXiv:1906.06532*, 2019.
- [37] X. Zhang, H. Liu, Q. Li, and X.-M. Wu, “Attributed graph clustering via adaptive graph convolution,” in *Proceedings of the 28th International Joint Conference on Artificial Intelligence*, 2019, pp. 4327–4333.
- [38] J. Park, M. Lee, H. J. Chang, K. Lee, and J. Y. Choi, “Symmetric graph convolutional autoencoder for unsupervised graph representation learning,” in *Proceedings of the IEEE/CVF International Conference on Computer Vision*, 2019, pp. 6519–6528.
- [39] J. Cheng, Q. Wang, Z. Tao, D. Xie, and Q. Gao, “Multi-view attribute graph convolution networks for clustering,” in *Proceedings of the Twenty-Ninth International Conference on International Joint Conferences on Artificial Intelligence*, 2021, pp. 2973–2979.
- [40] Z. Peng, H. Liu, Y. Jia, and J. Hou, “Attention-driven graph clustering network,” in *Proceedings of the 29th ACM International Conference on Multimedia*, 2021, pp. 935–943.
- [41] S. Pan, R. Hu, G. Long, J. Jiang, L. Yao, and C. Zhang, “Adversarially regularized graph autoencoder for graph embedding,” in *Proceedings of the 27th International Joint Conference on Artificial Intelligence*, 2018, pp. 2609–2615.
- [42] Z. Tao, H. Liu, J. Li, Z. Wang, and Y. Fu, “Adversarial graph embedding for ensemble clustering,” in *International Joint Conferences on Artificial Intelligence Organization*, 2019.
- [43] G. Cui, J. Zhou, C. Yang, and Z. Liu, “Adaptive graph encoder for attributed graph embedding,” in *Proceedings of the 26th ACM SIGKDD International Conference on Knowledge Discovery & Data Mining*, 2020, pp. 976–985.
- [44] W. Xia, Q. Wang, Q. Gao, M. Yang, and X. Gao, “Self-consistent contrastive attributed graph clustering with pseudo-label prompt,” *IEEE Transactions on Multimedia*, 2022.
- [45] Y. Liu, X. Yang, S. Zhou, and X. Liu, “Simple contrastive graph clustering,” *arXiv preprint arXiv:2205.0786*, 2022.
- [46] Y. Liu, J. Xia, S. Zhou, S. Wang, X. Guo, X. Yang, K. Liang, W. Tu, Z. S. Li, and X. Liu, “A survey of deep graph clustering: Taxonomy, challenge, and application,” *arXiv preprint arXiv:2211.12875*, 2022.
- [47] T. Chen, S. Kornblith, M. Norouzi, and G. Hinton, “A simple framework for contrastive learning of visual representations,” in *International conference on machine learning*. PMLR, 2020, pp. 1597–1607.
- [48] J.-B. Grill, F. Strub, F. Altché, C. Tallec, P. H. Richemond, E. Buchatskaya, C. Doersch, B. A. Pires, Z. D. Guo, M. G. Azar *et al.*, “Bootstrap your own latent: A new approach to self-supervised learning,” *arXiv preprint arXiv:2006.07733*, 2020.
- [49] J. Zbontar, L. Jing, I. Misra, Y. LeCun, and S. Deny, “Barlow twins: Self-supervised learning via redundancy reduction,” *arXiv preprint arXiv:2103.03230*, 2021.
- [50] X. Chen and K. He, “Exploring simple siamese representation learning,” in *Proceedings of the IEEE/CVF Conference on Computer Vision and Pattern Recognition*, 2021, pp. 15 750–15 758.
- [51] K. Liang, Y. Liu, S. Zhou, X. Liu, and W. Tu, “Relational symmetry based knowledge graph contrastive learning,” *arXiv preprint arXiv:2211.10738*, 2022.
- [52] Y. Zhu, Y. Xu, F. Yu, Q. Liu, S. Wu, and L. Wang, “Deep Graph Contrastive Representation Learning,” in *ICML Workshop on Graph Representation Learning and Beyond*, 2020. [Online]. Available: <http://arxiv.org/abs/2006.04131>
- [53] Y. You, T. Chen, Y. Sui, T. Chen, Z. Wang, and Y. Shen, “Graph contrastive learning with augmentations,” *Advances in Neural Information Processing Systems*, vol. 33, pp. 5812–5823, 2020.
- [54] Y. Zhu, Y. Xu, Q. Liu, and S. Wu, “An empirical study of graph contrastive learning,” *arXiv preprint arXiv:2109.01116*, 2021.
- [55] Y. Zhu, Y. Xu, H. Cui, C. Yang, Q. Liu, and S. Wu, “Structure-enhanced heterogeneous graph contrastive learning,” in *Proceedings of the 2022 SIAM International Conference on Data Mining (SDM)*. SIAM, 2022, pp. 82–90.
- [56] Y. Liu, S. Zhou, X. Liu, W. Tu, and X. Yang, “Improved dual correlation reduction network,” *arXiv preprint arXiv:2202.12533*, 2022.
- [57] L. Yu, S. Pei, L. Ding, J. Zhou, L. Li, C. Zhang, and X. Zhang, “Sail: Self-augmented graph contrastive learning,” in *Proceedings of the AAAI Conference on Artificial Intelligence*, vol. 36, no. 8, 2022, pp. 8927–8935.
- [58] Y. Wang, W. Wang, Y. Liang, Y. Cai, J. Liu, and B. Hooi, “Nodeaug: Semi-supervised node classification with data augmentation,” in *Proceedings of the 26th ACM SIGKDD International Conference on Knowledge Discovery & Data Mining*, 2020, pp. 207–217.
- [59] Y. Wang, W. Wang, Y. Liang, Y. Cai, and B. Hooi, “Mixup for node and graph classification,” in *Proceedings of the Web Conference 2021*, 2021, pp. 3663–3674.

- [60] N. Lee, J. Lee, and C. Park, "Augmentation-free self-supervised learning on graphs," *arXiv preprint arXiv:2112.02472*, 2021.
- [61] Y. Zhu, Y. Xu, F. Yu, Q. Liu, S. Wu, and L. Wang, "Graph contrastive learning with adaptive augmentation," in *Proceedings of the Web Conference 2021*, 2021, pp. 2069–2080.
- [62] Y. Wang, Y. Cai, Y. Liang, H. Ding, C. Wang, S. Bhatia, and B. Hooi, "Adaptive data augmentation on temporal graphs," *Advances in Neural Information Processing Systems*, vol. 34, pp. 1440–1452, 2021.
- [63] W. Jin, X. Liu, X. Zhao, Y. Ma, N. Shah, and J. Tang, "Automated self-supervised learning for graphs," *arXiv preprint arXiv:2106.05470*, 2021.
- [64] M. Defferrard, X. Bresson, and P. Vandergheynst, "Convolutional neural networks on graphs with fast localized spectral filtering," *Advances in neural information processing systems*, 2016.
- [65] J. A. Hartigan and M. A. Wong, "Algorithm as 136: A k-means clustering algorithm," *Journal of the royal statistical society. series c (applied statistics)*, vol. 28, no. 1, pp. 100–108, 1979.
- [66] X. Yang, X. Hu, S. Zhou, X. Liu, and E. Zhu, "Interpolation-based contrastive learning for few-label semi-supervised learning," *IEEE Transactions on Neural Networks and Learning Systems*, pp. 1–12, 2022.
- [67] Y. Zhu, Y. Xu, F. Yu, Q. Liu, S. Wu, and L. Wang, "Deep graph contrastive representation learning," *arXiv preprint arXiv:2006.04131*, 2020.
- [68] Y. Zhu, Y. Xu, Q. Liu, and S. Wu, "An empirical study of graph contrastive learning," *arXiv preprint arXiv:2109.01116*, 2021.
- [69] X. Yang, Y. Liu, S. Zhou, X. Liu, and E. Zhu, "Interpolation-based correlation reduction network for semi-supervised graph learning," *arXiv preprint arXiv:2206.02796*, 2022.
- [70] J. Xie, R. Girshick, and A. Farhadi, "Unsupervised deep embedding for clustering analysis," in *International conference on machine learning*. PMLR, 2016, pp. 478–487.
- [71] B. Yang, X. Fu, N. D. Sidiropoulos, and M. Hong, "Towards k-means-friendly spaces: Simultaneous deep learning and clustering," in *international conference on machine learning*. PMLR, 2017, pp. 3861–3870.
- [72] X. Li, H. Zhang, and R. Zhang, "Adaptive graph auto-encoder for general data clustering," *IEEE Transactions on Pattern Analysis and Machine Intelligence*, 2021.
- [73] L. Gong, S. Zhou, X. Liu, and W. Tu, "Attributed graph clustering with dual redundancy reduction," in *IJCAI*, 2022.
- [74] B. Fatemi, L. El Asri, and S. M. Kazemi, "Slaps: Self-supervision improves structure learning for graph neural networks," *Advances in Neural Information Processing Systems*, vol. 34, pp. 22 667–22 681, 2021.
- [75] Y. Liu, Y. Zheng, D. Zhang, H. Chen, H. Peng, and S. Pan, "Towards unsupervised deep graph structure learning," in *Proceedings of the ACM Web Conference 2022*, 2022, pp. 1392–1403.
- [76] N. Mrabah, M. Bouguessa, M. F. Touati, and R. Ksantini, "Rethinking graph auto-encoder models for attributed graph clustering," *arXiv preprint arXiv:2107.08562*, 2021.
- [77] S. Zhou, X. Liu, M. Li, E. Zhu, L. Liu, C. Zhang, and J. Yin, "Multiple kernel clustering with neighbor-kernel subspace segmentation," *IEEE transactions on neural networks and learning systems*, vol. 31, no. 4, pp. 1351–1362, 2019.
- [78] S. Wang, X. Liu, X. Zhu, P. Zhang, Y. Zhang, F. Gao, and E. Zhu, "Fast parameter-free multi-view subspace clustering with consensus anchor guidance," *IEEE Transactions on Image Processing*, vol. 31, pp. 556–568, 2021.
- [79] S. Wang, X. Liu, L. Liu, S. Zhou, and E. Zhu, "Late fusion multiple kernel clustering with proxy graph refinement," *IEEE Transactions on Neural Networks and Learning Systems*, 2021.
- [80] T. N. Kipf and M. Welling, "Variational graph auto-encoders," *arXiv preprint arXiv:1611.07308*, 2016.
- [81] E. Pan and Z. Kang, "Multi-view contrastive graph clustering," *Advances in neural information processing systems*, vol. 34, pp. 2148–2159, 2021.
- [82] L. Van der Maaten and G. Hinton, "Visualizing data using t-sne." *Journal of machine learning research*, vol. 9, no. 11, 2008.